Special Feature: Applied Nanoscale Morphology

Research Report

Stacking Structure of Silicon Nanosheets and Their Electron Transport Properties

Hideyuki Nakano and Takashi Ikuno

Report received on Mar. 5, 2014

ABSTRACT Low-dimensional silicon nanomaterials are promising candidates for applications in photonic, electronic, and biosensing devices by virtue of their size-dependent quantum effects. In particular, two-dimensional nanosheet structures can be used in conventional planar devices. However, there is no example of successful synthesis of two-dimensional silicon nanomaterials with large lateral size and oxide-free surfaces. Here we report that silicon nanosheets (SiNSs) covered with organic groups can be obtained by exfoliation of layered polysilane as a result of reaction with organic moieties. The organic moieties are covalently bound to the Si(111) planes. Amine-modified layered polysilane can be dissolved in chloroform and exfoliate into nanosheets that are 1-2 μm wide in the lateral direction and with thicknesses on the order of nanometers. The nanosheets have very flat and smooth surfaces due to dense coverage of organic moieties, and they are easily self-assembled in a concentrated state to form a regularly stacked structure. We have characterized the electron transport properties of organic-functionalized SiNSs using atomic force microscopy with a conductive cantilever under vacuum conditions at room temperature. Electrons are transported from the cantilever to the substrate through the SiNSs. The SiNSs exhibited nonresonant tunneling; the transport mechanisms are based on direct tunneling at low bias voltages and Fowler–Nordheim tunneling at high bias voltages.

KEYWORDS Silicon Nanosheets, Electron Transport, Two-dimensional Nano-materials, Surface Modification, Exfoliation

1. Introduction

Two-dimensional semiconductor nanosheets[1-4] can be potentially employed as building blocks for future nanodevices such as sensors, solar cells, and batteries, because of their unique physical and chemical properties. NSs have thicknesses that are typically on the order of nanometers, which are less than 1/100 of their lateral dimensions; their distinctive properties are attributable to their anisotropic geometry. From the viewpoint of applications, NSs must be highly compatible with planar integrated circuits and be easily fabricated via microprocessing techniques. Accordingly, NSs made of Si are suitable for conventional Si-based integrated circuits.[5]

Takeda et al. investigated the electronic structure of one-dimensional (1D) and two-dimensional (2D) Si-skeleton materials. They indicated that the 2D material has a unique band structure, which is intermediate between direct (1D) and indirect (3D).[6] The structure and photoluminescence properties of the layered silicon compounds were investigated by Stutzmann et al.[7] Based on these previous works, SiNSs are believed to represent a different framework material with physical characteristics contrasting those of the more conventional bulk, thin-film, and nanocrystalline forms.[8]

We have recently fabricated oxygen-free SiNSs[9,10] by the exfoliation of layered polysilane.[11,12] These SiNSs are soluble in organic solvents and are likely to be parallel to the substrate surface. Thus, they are potentially useful for a wide range of applications. The structural, optical, and electronic properties of SiNSs have been intensively investigated.[9,10] Recently, the macroscopic electronic properties of SiNS aggregates were investigated using photocurrent measurements.[7] However, the microscopic electronic properties of single-layer SiNSs (e.g., their electron transport properties) have not been characterized extensively. It is critical to determine the fundamental properties of SiNSs before they can be utilized in applications. We have attempted to do this in the present

© Toyota Central R&D Labs., Inc. 2014

work. To the best of our knowledge, this study is the first investigation of the electron transport properties of single layer SiNSs. Atomic force microscopy (AFM) with a conductive cantilever was adopted to confirm the number of SiNS layers and to obtain the current-voltage (*I*-*V*) plots.

2. Results and Discussions

2. 1 Alkyl-modified SiNSs

Layered polysilane (Si_6H_6) was prepared according to the method described by Yamanaka et. al.[13] Si_6H_6 (**Fig. 1**(a)) was functionalized with hexyl chains using a Pt-catalyzed hydrosilylation reaction with 1-hexene to produce a stable colloidal suspension (Fig. 1(b)). The obtained material (Hex.-SiNS) is soluble in typical organic solvents such as hexane, chloroform, acetone, and diethyl ether, and is insoluble in water and ethanol. Fourier transform-infrared (FT-IR) spectroscopy was used to identify and characterize the organic species on the silicon surface.

Figure 2(a) shows the attenuated total reflection (ATR) IR spectrum for Hex.-SiNS. The spectrum contains alkyl stretching and bending absorptions between 2856 and 2954 cm^{-1} and between 1259 and 1459 cm^{-1}, respectively. In addition, a peak attributable to Si-CH_2 vibrational scissoring was observed at 729 cm^{-1}. The presence of characteristic vibrations for

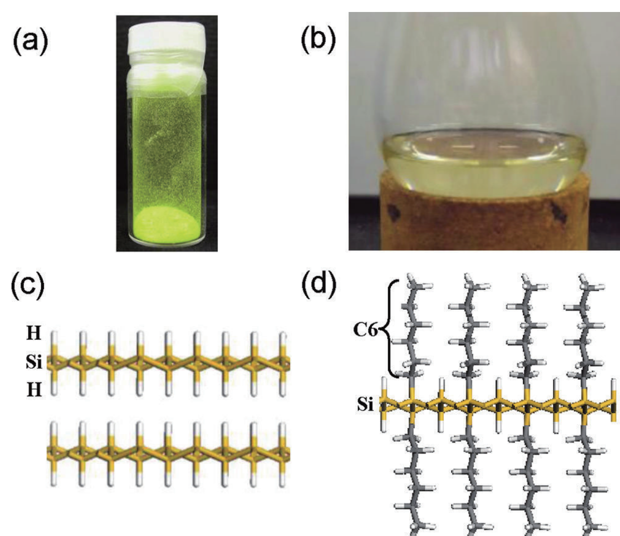

Fig. 1 (a) Photograph and (c) structure of Si_6H_6.
(b) Photograph and (d) structure of Hex.-SiNS.

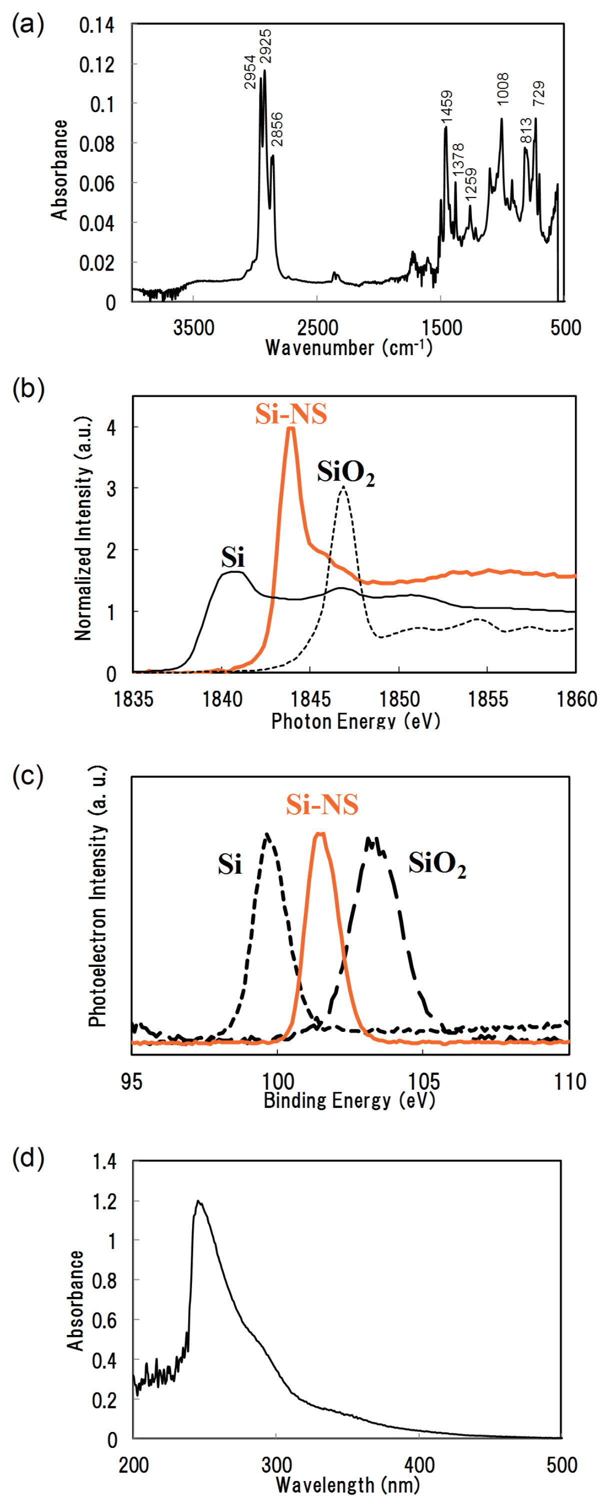

Fig. 2 (a) FTIR spectra of Hex.-SiNS. (b) Si K-edge XANES spectra of Hex.-SiNS (brown line), Si(111) wafer and SiOx (black line). The data were recorded at beam line BL-10 in the Ritsumeikan SR Center. (c) XPS Si 2p spectra of Hex.-SiNS (brown line), Si(111) wafer and SiOx (black line). (d) UV spectrum of Hex.-SiNS.

© Toyota Central R&D Labs., Inc. 2014

organic molecules in Hex.-Si after the reaction, along with a reduction in the intensity of the Si-H peak at 2110 cm^{-1} and the absence of peaks characteristic of a terminal double bond (C-C; 1600 cm^{-1}), indicate that the organic molecules were covalently attached to the silicon surface. Although the peaks between 1000 and 1100 cm^{-1} correspond to Si-OR stretching vibrations, the relatively low magnitude of these peaks indicates that oxidation of Hex.-Si was minimal.

The local environment of the silicon framework was examined using X-ray absorption near edge structure (XANES) analysis. The Si K-edge absorption spectra are compared with those for a (111) oriented p-type silicon wafer and amorphous SiO_2 in Fig. 2(b). The prominent peak at 1847 eV for SiO_2 arises primarily from Si 1s→ O 2p transitions and is shifted by 7 eV to higher energy compared to the bulk Si edge due to the more positively charged Si in SiO_2. This peak serves as a sensitive fingerprint to identify and estimate the amount of SiO_2-like species present in the sample. XANES from Hex.-SiNS exhibits features at an energy of 1844 eV, which is between those measured for the Si and SiO_2 samples. After oxidation of Hex.-SiNS with water over a 10 day period, a new peak at 1847 eV was observed, which corresponds to SiO_2 and suggests the generation of a suboxide SiO_x species in the sheet framework. Thus, the peak at 1844 eV is assigned to the Si-C bond, which is the same bond energy as that for a tetra-coordinated silicon atom-bonded organic group.

Next, the oxidation state of Si in Hex.-SiNS was probed using X-ray photoelectron spectroscopy (XPS). The XPS spectrum displayed a Si 2p peak with a binding energy of 102.0 eV (Fig. 2(c)), which suggests that only one site exists in the structure. The Si 2p spectra obtained from bulk Si (99.0 eV) and SiO_2 (104 eV) are very different from those of Hex.-SiNS, which is not simply due to a mixture of Si and SiO_2. Recently, XPS data for decyl-capped silicon nanocrystals was reported, in which the peaks at 99 and 102 eV were attributed to the silicon core and surface Si-organo group and oxides, respectively.[14] Although no peak was observed at 99 eV in Hex.-SiNS, the peak at 102 eV indicates that Hex.-SiNS does not have a core, but a bond attributed to a Si-organo group. This is evidence for the successful preparation of Hex.-SiNS. The color of the hexane suspension of Hex.-SiNS was light-brown (Fig. 1(b)), depending on the amount of Si, and it exhibited optical properties that differed from the starting materials of Si_6H_6. There was a clear and substantial blue-shift of the absorption edge of Hex.-SiNS relative to Si_6H_6. More specifically, the absorption associated with the bandgap transition occurred at 4.2 eV for Hex.-SiNS (Fig. 2(d)), which is a shorter wavelength than that for bulk silicon (1.1 eV)[15] and Si_6H_6 (2.3 eV).[14] The bandgap is in good agreement with the theoretical direct bandgap for Si_6H_6 of 3 eV.[16] The absorption spectrum indicates the monolayer nature of the sheet, reflecting dispersion into Hex.-SiNS in the organic solvent. Furthermore, this marked blue shift can be understood by considering the changes in the density of the electron energy states due to the sub-nanometer thickness of Hex.-SiNS. Physicochemical investigation of semiconductor nanosheets is expected to become a fertile ground for future research, and lead to novel applications of such two-dimensional silicon networks.

2. 2 Regular Stacking Structure of SiNSs

The amination of Si_6H_6 was performed in an inert atmosphere according to the previously reported method.[9] Internal structures in the agglomerated state of n-decylamine (C10) -SiNS and other amine modified Si nanosheets were detected by XRD. Samples were prepared by dropping solutions of C10-SiNS in chloroform onto a glass plate, followed by volatilization of the solvent. A very strong narrow peak at $2\theta = 2.96°$, which corresponds to $q = 2.11$ nm^{-1} in the wavenumber vector [$q = (4\pi/\lambda) \sin \theta$] scale, was observed for C10-SiNS (**Fig. 3(**a)). This peak is related to the interlayer distance ($d = 2.98$ nm) of the nanosheets and appears together with its higher order peaks, which can be assigned as (00*l*) planes. No other peaks were observed. This diffraction peak is associated with stacking of the nanosheets. Thus, the nanosheets agglomerate in a concentrated state to form a regularly stacked structure by self-assembly. Although C10-SiNS is oxidized in air, the XRD peaks remained and did not disappear easily after the samples were exposed to air; therefore, the interior of the agglomerate is assumed to have oxidation resistance and maintains the regularly stacked structure.

The peak associated with (001) planes is much sharper than that for Si_6H_6 (Fig. 3(e)). The broadness of the latter peak is attributed to the small crystallite size, in which approximately 10 layers are included.[17] The strong sharp peak for the C10-SiNS indicates

© Toyota Central R&D Labs., Inc. 2014

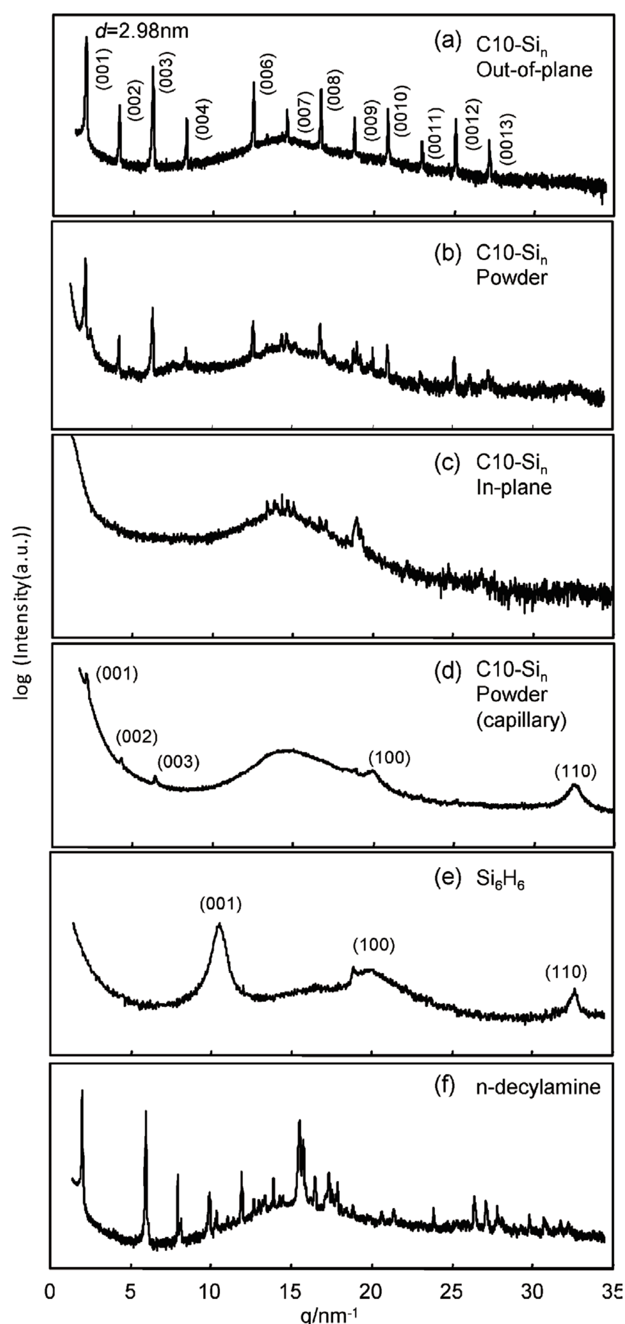

Fig. 3 XRD patterns for (a-d) C10-SiNS and those for (e) Si_6H_6 and (f) n-decylamine for comparison. (a) Out-of-plane, (b) powder, and (c) in-plane patterns of the C10-SiNS layered sample wherein silicon layers are stacked parallel to the surface of the glass plate. (d) Pattern measured using a powder sample filled in a glass capillary. Patterns (c) and (d) were measured using synchrotron radiation, and parts of the samples were destroyed during the measurements.

multilayer stacking consisting of several tens of layers. In contrast to the out-of-plane pattern, several additional peaks appear at $q > 13$ nm^{-1} in the XRD pattern for the C10-SiNS powder sample (Fig. 3(b)). These peaks also appear in the in-plane XRD pattern for the sample used for the in-plane measurement (Fig. 3(c)). The peaks are thought to be derived from ordered structures composed of *n*-decylamine residues on silicon layers, although peak assignments will be investigated in more detail in the near future. The alkyl chains in stacked C10-SiNS are thought to be aligned differently from those in *n*-decylamine crystals (Fig. 3(f)), due to binding to the silicon layers. The value of d = 2.98 nm suggests that the *n*-decylamine residues on the corrugated silicon layers are almost perpendicular to the layers with an extended chain conformation (**Fig. 4**). The remaining 2D silicon crystal structure was confirmed by XRD measurement of the C10-SiNS powder filled in glass capillaries (Fig. 3(d)). Peaks corresponding to the (100) and (110) planes of the corrugated silicon sheet are observed around q values of 20.4 and 32.8 nm^{-1}, respectively. A few peaks corresponding to the (00*l*) planes of C10-SiNS are also observed, although higher order peaks are absent, due to destruction of the *n*-decylamine residues by synchrotron radiation. The absence of peaks corresponding to the (001) planes of Si_6H_6 and $CaSi_2$ confirms that the peaks due to the (100) and (110) planes are derived from the two-dimensional silicon crystals included in C10-SiNS. A broad peak corresponding to (110) planes also appears in Fig. 3(b).

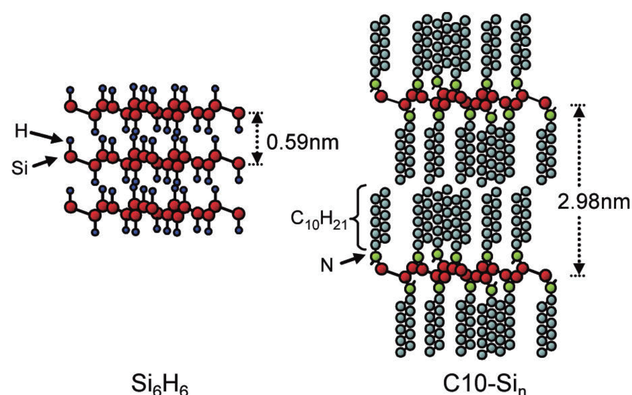

Fig. 4 Structural models of Si_6H_6 and regularly stacked C10-SiNS.

© Toyota Central R&D Labs., Inc. 2014

3. Electron Transport Properties of SiNSs

Figure 5(a) shows AFM images of C10-SiNS dispersed on a HOPG surface. We observed sheet-like structures, indicating that the C10-SiNSs were deposited parallel to the HOPG surface. The lateral dimensions of the C10-SiNSs were typically in the range of 50 to 300 nm. The heights of the NSs labeled A, B, and C in Fig. 5(a) obtained from line profiles (Fig. 5(b)) are around 3 nm. Since single-layer SiNSs have been estimated to be 2.98 nm thick (see inset of Fig. 5(b)), the C10-SiNSs A, B, and C are single layers.

Figure 6 shows the *I-V* characteristics of the C10-SiNSs A, B and C immediately after obtaining the topographs. Current flowed at voltages in the range of 0 to 1 V. For C10-SiNSs A and B, the voltage was swept once, while for the C10-SiNS C, *I-V* curves were obtained at the same point three times. All *I-V* curves exhibited similar nonlinear shapes. However, the currents were slightly different due to fluctuations in the contact area of the cantilever and the C10-SiNSs. For the C10-SiNS C, the three *I-V* curves had almost the same shape. In the voltage range from 0 to 1 V, the C10-SiNSs are relatively stable and show similar *I-V* characteristics. Above 1 V, breakdown occasionally occurred; a larger current was measured in the next voltage sweep, indicating that the C10-SiNSs had been destroyed. Although the effect of the applied electric field on mechanical deformation in the C10-SiNSs was not clarified, we infer that the strong local electric field formed by the sharp cantilever as an electrode might break the C10-SiNSs at high bias voltages.

As the Si(111) atomic layer is comprised of a periodic structure of Si atoms (see the inset of Fig. 5(b)) and is the fundamental structure in the C10-SiNSs, it is expected that the C10-SiNSs have a band structure.(18) Organic molecules adsorbed on the Si(111) layers might create potential barriers against the band edges of Si(111), leading to a C10-SiNS which has a double-barrier quantum-well structure.(19) However, it is unlikely that electrons tunnel through the confinement level in the quantum well (i.e., resonant tunneling) because the confinement level is too high due to the ultrathin Si(111). Therefore, we can conclude that the C10-SiNSs functionalized by organic molecules possibly act as a single potential barrier.

We believe that the *I-V* curves for the C10-SiNSs can be modeled by an arbitrary tunnel barrier within the Simmons approximation,(20) which is the simplest way to model the *I-V* curves of a metal-insulator-metal system. **Figure 7**(a) shows the energy diagrams for the cantilever/C10-SiNSs/HOPG system at different bias voltages. When the applied voltage is less than the barrier height ϕ (the energy offset between the electrode Fermi level (E_F) and the NS conduction band minimum (CBM)), electrons tunnel through a trapezoidal barrier,(24) i.e., direct tunneling occurs. When the applied voltage exceeds ϕ, electrons tunnel through a triangular barrier, which is analogous to field emission and Fowler–Nordheim (FN) tunneling(21) occurs. The relationship between the tunneling current

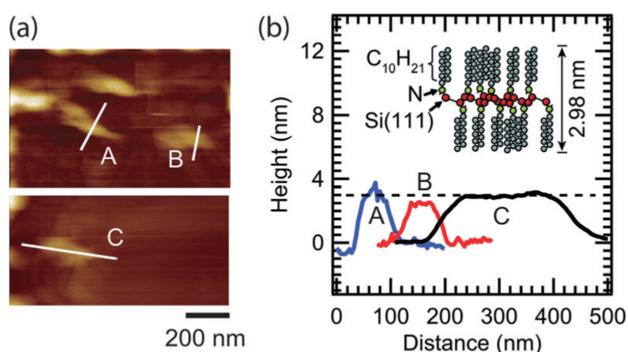

Fig. 5 (a) AFM images of C10-SiNSs dispersed on a HOPG substrate. The scale bar is 200 nm. (b) Line profiles of the heights of the NSs at points A, B, and C indicated in (a). Inset: Schematic illustration of single-layer C10-SiNS. Maximum heights of the line profiles of A, B, and C correspond to the monolayer heights.

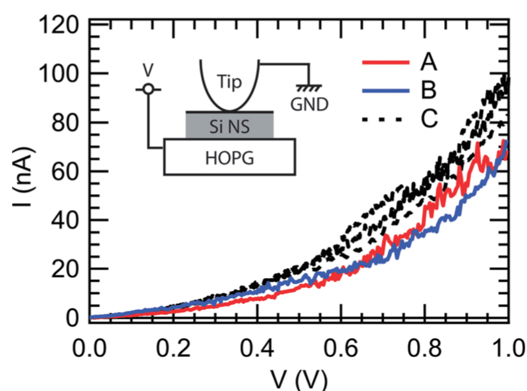

Fig. 6 *I-V* curves for C10-SiNSs A, B, and C, shown in Fig. 5(a). Inset: Schematic illustration of the experimental setup for electron transport measurement.

© Toyota Central R&D Labs., Inc. 2014

I and the applied bias voltage V is expressed by the following equations:[22]

$$I \propto \begin{cases} V \exp\left(-\dfrac{2d\sqrt{2m^*\phi}}{\hbar}\right) & (V < V_{trans}): \textit{Direct tunneling} \\ V^2 \exp\left(-\dfrac{4d\sqrt{2m^*\phi^3}}{3\hbar eV}\right) & (V > V_{trans}): \textit{FN tunneling} \end{cases} \quad (1)$$

where m^* is the effective mass of the electron, e is the elementary electronic charge, $\hbar$ is Planck's constant, and d is the C10-SiNS thickness.

The transition voltage from direct tunneling to FN tunneling, V_{trans}, can be defined as $V_{trans} = \phi/e$. V_{trans} can be determined from a plot of $\ln(I/V^2)$ against $(1/V)$ (i.e., an FN plot) when Eq. (1) is rewritten as

$$\ln\left(\frac{I}{V^2}\right) \propto \begin{cases} \ln\left(\dfrac{1}{V}\right) & (V < V_{trans}): \textit{Direct tunneling} \\ -\left(\dfrac{1}{V}\right) & (V > V_{trans}): \textit{FN tunneling} \end{cases} \quad (2)$$

Figure 7(b) shows an FN plot of the C10-SiNS (NS A) and its fitting curve. The experimental plot contains an inflection point. Other C10-SiNSs also showed similar inflection points in the FN plots (data not shown). The inflection point at about $1/V \approx 2.0[V^{-1}]$ divides the plot into two regimes. The fitting curve based on Eq. (2) in Fig. 7(b) exhibits good agreement with the experimental plot. A linear decrease at high bias voltage and logarithmic growth at low bias voltage indicates that the transport mechanisms in C10-SiNS are based on direct tunneling and FN tunneling at low bias voltages and high bias voltages, respectively. V_{trans} can be derived from the position of the inflection point in Fig. 7(b). The average value of V_{trans} obtained from the FN plots of all data curves in Fig. 6 for single-layer C10-SiNSs was 0.54 V. Thus, the barrier height ϕ should be 0.54 eV for the combination of a PtIr electrode (cantilever) and the C10-SiNS.

Even though the C10-SiNSs used in this study have alkanes on their surfaces, they showed smaller V_{trans} values than al kane molecules ($V_{trans} \approx 1.2$ V) as reported by Beebe et al.[23] Note that since the electrode material PtIr[24] has a similar work function as Au, which Beebe et al. used, it is possible to directly compare our results with theirs. The reason why the C10-SiNSs have a smaller V_{trans} than alkane molecules might be because the barrier height ϕ of the C10-SiNSs is smaller than the difference between E_F and the lowest unoccupied molecular orbital (LUMO) of the alkane. In fact, we previously found that the optical band gap of C10-SiNSs was approximately 2.8 eV, which is much smaller than the highest occupied molecular orbital (HOMO)-LUMO gap of alkanes (7-8 eV).[25] This difference might also affect the difference in V_{trans}.

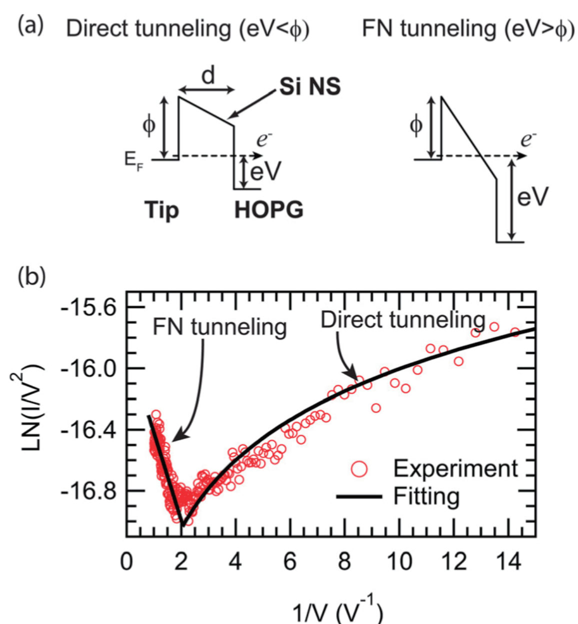

Fig. 7 (a) Schematic illustrations of the barrier shapes at eV < ϕ, and eV > ϕ, corresponding to direct tunneling and Fowler-Nordheim tunneling, respectively.
(b) Fowler-Nordheim plot of the C10-SiNS. Fitting curves are also given (solid line). The data clearly show two tunneling regimes depending on the applied bias voltage.

4. Conclusion

We have demonstrated a successful method for the synthesis of organo-modified SiNSs incorporating different functional groups, and we also were able to measure the electron transport properties of single-layer SiNSs for the first time. These new silicon structures with the surface bonded to alkyl groups enable uniform dispersion in organic solvents. Therefore, polycrystalline silicon films for new types of sensors or other novel nanostructured devices can be prepared on any substrate by spin-coating of the sheet suspension at close to room temperature. It was found that the electron transport mechanism in spin-coated C10-SiNSs is based on nonresonant tunneling. At applied voltages of less than V_{trans} (0.54 V), direct tunneling was dominant,

© Toyota Central R&D Labs., Inc. 2014

whereas FN tunneling was dominant at voltages greater than Vtrans. This value is smaller than that for alkane molecules, indicating that the barrier height ϕ of the C10-SiNSs is smaller than that of the molecule. This implies that it may be possible to tune the electronic structures of the SiNSs by varying the functionalized molecules. SiNSs with tunable electronic structures might be suitable for barrier layers or well layers in superlattice devices such as light-emitting devices, ultrafast switching devices, and sensors. To achieve these applications, it is essential to precisely control the geometrical structure, the number of layers, and positioning of the SiNSs on a substrate.

References

(1) Sasaki, T. and Watanabe, M., *J. Phys. Chem. B*, Vol. 101 (1997), pp. 10159-10161.
(2) Yan, C. and Xue, D., *J. Phys. Chem. B,* Vol. 109 (2005), pp. 12358-12361.
(3) Hosono,E., Fujihara, S., Honna, I. and Zhou, H. S., *Adv. Mater.*, Vol. 17 (2005), pp. 2091-2094.
(4) Sasaki, T., *J. Ceram. Soc. Jpn.,* Vol. 115, No. 1337 (2007), pp. 9-16.
(5) Sze, S. M., *Semiconductor Devices, Physics and Technology* (2002), John Wiley & Sons, Inc.
(6) Takeda, K. and Shiraishi, K., *Phys. Rev. B,* Vol. 39, No. 15 (1989), 11028.
(7) Stutzmann, M., Brandt, M. S., Rosenbauer, M., Fuchs, H. D., Finkbeiner, S., Weber, J. and Deak, P., *J. of Lumin.,* Vol. 57, No. 1-6 (1993), pp. 321-330.
(8) Brus, L., *J. of Phys. Chem.*, Vol. 98, No. 14 (1994), pp. 3575-3581.
(9) Okamoto, H., Kumai, Y., Sugiyama, Y., Mitsuoka, T., Nakanishi, K., Ohta, T., Nozaki, H., Yamaguchi, S., Shirai, S. and Nakano, H., *J. Am. Chem. Soc.,* Vol. 132 (2010), pp. 2710-2718.
(10) Sugiyama, Y., Okamoto, H., Mitsuoka, T., Morikawa, T., Nakanishi, K., Ohta, T. and Nakano, H., *J. Am. Chem. Soc.,* Vol. 132 (2010), pp. 5946-5947.
(11) Nakano, H., Mitsuoka, T., Harada, M., Horibuchi, K., Nozaki, H., Takahashi, N., Nonaka, T., Seno, Y. and Nakamura, H., *Angew. Chem. Int. Ed.,* Vol. 45, No.38 (2006), pp. 6303-6306.
(12) Nakano, H., Ishii, M. and Nakamura, H., *Chem. Commun.*, (2005), pp. 2945-2947.
(13) Yamanaka, S., Matsu-ura, H. and Ishikawa, M., *Mat. Res. Bull.*, Vol. 31, No. 3 (1996), pp. 307-316.
(14) Mastronardi, M. L., Hennrich, F., Henderson, E. J., Maier-Flaig, F., Blum, C., Reichenbach, J., Lemmer, U., Kübel. C., Wang, D., Kappes, M. M. and Ozin, G. A., *J. Am. Chem. Soc.,* Vol. 133, No. 31 (2011), p. 11928-11931.
(15) Wilcoxon, J. P., Samara, G. A. and Provencio, P. N., *Phys. Rev. B,* Vol. 60, No.4 (1999), pp. 2704-2714.
(16) He, J., Tse, J. S., Klug, D. D. and Preston, K. F., *J. Mat. Chem.,* Preston, Vol. 8, No. 3 (1998), pp. 705-710.
(17) Dahn, J. R., Way, B. M., Fuller, E. and Tse, J. S., *Physical Review B,* Vol. 48, No. 24 (1993), pp. 17872-17877.
(18) Tse, J. S., Dahn, J. R. and Buda, F., *J. Phys. Chem.,* Vol. 99 (1995), pp. 1896-1899.
(19) Mizuta, H. and Tanoue, T., *The Physics and Applications of Resonant Tunneling Diodes* (1995), Cambridge University Press, Cambridge.
(20) Simmons, J. G., *J. Appl. Phys.,* Vol. 34 (1963), pp. 1793-1803.
(21) Gomer, R., *Field Emission and Field Ionization,* (1993), American Institute of Physics, New York.
(22) Beebe, J. M., Kim, B. S., Gadzuk, J. W., Frisbie, C. D. and Kushmerick, J. G., *Phys. Rev. Lett.*, Vol. 97 (2006), 026801.
(23) Beebe, J. M., Kim, B. S., Frisbie,C. D. and Kushmerick, J. G., *ACS Nano*, Vol. 2, No. 5 (2008), pp. 827-832.
(24) Spadafora, E. J., Demadrille, R., Ratier, B. and Grévin, B., *Nano Lett.,* Vol. 10 (2010), pp. 3337-3342.
(25) Salomon, A., Cahen, D., Lindsay, S., Tomfohr, J., Engelkes, V. B. and Frisbie, C. D., *Adv. Mater.,* Vol. 15 (2003), pp.1881-1890.

Figs. 1 and 2
Reprinted from J. Am. Chem. Soc., Vol. 134 (2012), pp. 5452-5455, Nakano, H., Nakano, M., Nakanishi, K., Tanaka, D., Sugiyama, Y., Ikuno, T., Okamoto, H. and Ohota, T., Preparation of Alkyl-Modified Silicon Nanosheets by Hydrosilylation of Layered Polysilane (Si_6H_6), © 2012, with permission from American Chemical Society.

Figs. 3 and 4
Reprinted from J. Am. Chem. Soc., Vol. 132 (2010), pp. 2710-2718, Okanoto, H., Kumai, Y., Sugiyama, Y., Mitsuoka, T., Nakanishi, K., Ohta, T., Nozaki, H., Yamaguchi, S., Shirai, S. and Nakano, H., Silicon Nanosheets and Their Self-assembled Regular Stacking Structure, © 2012, with permission from American Chemical Society.

Figs. 5-7
Reprinted from Appl. Phy. Lett., Vol. 99 No. 2 (2011), 023107, Ikuno, T., Okamoto, H., Sugiyama, Y., Nakano, H., Yamada, F. and Kamiya, I., Electron Transport Properties of Si Nonoshieets: Transition from Direct Tunneling to Fowler-Nordheim Tunneling, © 2011, with permission from American Institute of Physics.

Text
Partially adapted from J. Am. Chem. Soc., Vol. 132 (2010), pp. 2710-2718 and Vol. 134 (2012), pp. 5452-5455, © 2010 and 2012 American Chemical Society, with permission from American Chemical Society.

Hideyuki Nakano
Research Fields:
- Low-dimensional Semi-conductive Materials
- Energy Storage Materials

Academic Degree: Dr.Eng.
Academic Societies:
- The Ceramic Society of Japan
- The Chemical Society of Japan

Award:
- The Ceramic Society of Japan Award for Creative Work, 2013

Takashi Ikuno
Research Fields:
- Nanoelectronics
- Nanomaterials
- Photovoltaics

Academic Degree: Dr.Eng.
Academic Societies:
- The Japan Society of Applied Physics
- The Optical Society of Japan
- Materials Research Society

© Toyota Central R&D Labs., Inc. 2014